Available online at www.sciencedirect.com
SCIENCE DIRECT®
Proceedings of the Combustion Institute 30 (2005) 1467–1475
Proceedings of the Combustion Institute
www.elsevier.com/locate/proci

Monte-Carlo simulation of soot particle coagulation and aggregation: the effect of a realistic size distribution

Michael Balthasar[a,*], Michael Frenklach[b]

[a] Department of Chemical Engineering, University of Cambridge, Cambridge CB2 3RA, UK
[b] Department of Mechanical Engineering, University of California, Lawrence Berkeley National Laboratory, Berkeley, CA 94720-1740, USA

Abstract

The evolution of the morphology of primary soot particles was investigated in a laminar premixed flame with the emphasis on the effect of a realistic particle size distribution. A time-dependent Monte-Carlo method was used to calculate flame trajectories of single particles. In the nucleation zone of the flame, particles were grown by coagulation and simultaneous surface growth. The particles for coagulation were selected according to a pre-calculated size distribution obtained by solving the dynamics of the entire soot particle ensemble. In the post-nucleation zone, defined by the point of transition from coalescent to aggregate growth, only surface growth was applied to the particles. The simulation results provide further support to the notion that particle nucleation and the presence of small particles influence the morphology of primary particles and the location of transition. It is demonstrated that the mean size of subparticles comprising the primary particles is substantially smaller when using a realistic size distribution in the nucleation zone of the investigated flame. This, in turn, reduces the degree of aggregation of the primary particles at the time of transition to an extent that surface growth is able to recover their spherical shape in the post-nucleation zone.

Keywords: Soot formation; Particle aggregation; Morphology; Monte-Carlo simulations

1. Introduction

Carbonaceous soot particles emitted from practical combustion devices and flames are often characterized as fractal-like aggregates [1–7]. Individual aggregates are composed of spheroidal primary particles, varying in number and size depending on the conditions of the combustion system. The size of primary particles noticeably exceeds that of particles incepted from the gaseous phase. It is therefore often argued that particle aggregation is preceded by a period of coalescent growth [8]. The mechanism of transition from coalescent to aggregate growth is still unclear. A better understanding of these processes is essential since key properties of soot particulates are a result of the morphology of both aggregates and primary particles.

For instance, recent research on the toxicity of carbon particles indicates that size and shape of particles emitted from diesel engines have a significant impact on their adverse health effects [9,10]. Equally important is the morphology of aggregates for the formation of carbon black. The size

* Corresponding author. Fax: +44 1223 334786.
E-mail address: mb404@cam.ac.uk (M. Balthasar).

1540-7489/$ - see front matter © 2004 The Combustion Institute. Published by Elsevier Inc. All rights reserved.
doi:10.1016/j.proci.2004.07.035

and shape of the particles in composite systems are the major features that determine the practical properties of carbon black [11].

The coalescent growth of particles was attributed to viscous forces between small particles [12–16], often referred to as sintering. While sintering is important for other materials such as silica, it provides a less convincing argument for carbonaceous soot since soot does not melt. It was also suggested that it is a result of simultaneous coagulation and surface growth [8,17–19]. Mitchell and Frenklach [20,21] investigated the mechanism of transition from coalescent to aggregate growth by calculating trajectories of individual collector particles using a dynamic Monte-Carlo method. They concluded that the morphology of aggregating particles is intimately related to both the surface deposition and particle nucleation rates.

In a follow-up study, Balthasar and Frenklach [22] investigated the aggregation characteristics of the ensemble of soot particles in premixed laminar flames using the method of moments. The simulations indicated, as in the previous studies [20,21], that the transition from coalescent to aggregate growth is closely correlated to the depletion of small, newly incepted particles.

The objective of the present work was to investigate further the key notion of the prior studies—the critical role of the small particles on the transition from coalescent to aggregate growth. Specifically, we focus on the effect of a realistic particle size distribution on the sphericity of primary particles. A dynamic Monte-Carlo method developed by Mitchell and Frenklach [20,21] is employed to study the evolution of the shape of primary particles in a premixed laminar flame of ethylene. The particle distribution is treated explicitly, and use is made of the transition location predicted by the simulations with the method of moments [22]. Shapes of individual primary particles and integral quantities describing the state of the particle ensemble are investigated by means of this approach.

2. Method

2.1. Flame environment

The trajectories of single particles, referred to as *collectors* [20,21], in a premixed laminar flame were investigated. The collector particle is surrounded by a two-phase flame environment consisting of gas-phase species and an ensemble of *candidate* soot particles. The parameters characterizing the environment were obtained by simulating the chemical and transport processes in the flame using the Premix computer code [23], which was modified to include transport equations for the soot moments [24]. Gas-phase reactions were described by a detailed reaction mechanism [25,26], and the formation of soot particles was modeled with a kinetic soot model [25,27] based on the method of moments [28]. The soot model includes the processes of particle nucleation, coagulation, surface reactions, and particle aggregation [22]. Computed in this manner, temperature, particle number densities, mean particle diameters, and growth rates were expressed as functions of residence time.

2.2. Candidate particle size distribution

The properties described above provide a sufficient description of the growing environment when the size distribution of candidate particles is assumed monodispersed. To investigate the effect of small particles on the shape of evolving primary particles requires explicit knowledge of the particle size distribution. In the present study, the size distribution was calculated by solving the Smoluchowski master equations [29] with source terms added for nucleation and surface reactions

$$\frac{\partial N_i}{\partial t} = \frac{1}{2}\sum_{j=1}^{i-1}\beta_{j,i-j}N_jN_{i-j} - \sum_{j=1}^{\infty}\beta_{i,j}N_iN_j + k_{sg}S_{i-\Delta}N_{i-\Delta} - k_{sg}S_iN_i + \delta_{N_1}, \quad (1)$$

where N_i is the number density of particles of size class i, $\beta_{i,j}$ is the coagulation kernel valid for the entire range of Knudsen numbers [30], k_{sg} is the rate of surface growth, S_i is the surface area of particles of size class i, Δ is the number of carbon atoms added in a single surface growth event, and δ_{N_1} is the rate of nucleation with N_1 denoting that only the number density of the smallest size class is affected by nucleation. The smallest particles were assumed to be dimers of pyrene [31]. The first two terms on the right-hand side of Eq. (1) describe the gain and loss of particles of size class i due to coagulation, the third and fourth terms the surface growth, and the last term the nucleation. Other surface reactions, such as oxidation and condensation, were omitted in the present analysis as they are of secondary importance in the nucleation zone of the flame. Temperature as well as the rates of nucleation and surface growth obtained with the detailed kinetic soot model as described above were used as input. Numerical integration of Eq. (1) was accomplished using DVODE [32], an initial value problem ODE solver. The number of size classes was adjusted during the calculation to avoid the loss of large particles.

Simulations were performed in the nucleation zone of the flame corresponding to a residence time interval of 0–21 ms. The calculated size distribution was obtained at a set of time points and transformed according to

$$n(D) = \mathrm{d}N(\log D)/\mathrm{d}\log D, \quad (2)$$

where D is the diameter and N is the number density of the candidate particles. For each time point, the distribution was then fitted to a sum of a power-law and a log-normal distribution,

$$n(D) = aD^{-b} + \frac{c}{\sqrt{2\pi}\log\sigma} \times \exp\left[-\frac{(\log \mathrm{D} - \log\langle \mathrm{D}\rangle)^2}{2\log^2\sigma}\right], \quad (3)$$

which was found to be an accurate representation. Thus, the parameters a, b, c, σ, and $\langle D\rangle$ in Eq. (3) were obtained as functions of residence time and used as input to the Monte-Carlo simulations determining the size distribution of candidate particle at any instant of time in the interval from 0 to 21 ms.

2.3. Monte-Carlo simulations

The evolution of the size distribution of candidate particles completes the characterization of the growth environment of the collector particle. Thus, the environment is specified by the temperature, number density, surface growth rate, and the parameters of the candidate particle size distribution, all given as functions of residence time. Using these inputs, the evolution of collector particles was calculated with a Monte-Carlo method and code developed by Mitchell and co-workers [20,21,33]. The approach is based on a stochastic description of collisions of the collector particle with candidate particles.

In the Monte-Carlo simulations, the flame was divided into two zones: (a) the nucleation zone, where nucleation, coagulation, and surface reactions are all active, and (b) the post-nucleation zone, where only surface reactions act on the particles. The boundary between the two zones was determined by the transition time, 20.5 ms, taken from the numerical results obtained with a "complete" model using the method of moments [22]. In the present study, all particles in the distribution starting from 20.5 ms were referred to as primary particles. The objective is to investigate if these particles can recover a spherical shape if a realistic distribution of candidate particles is used in the nucleation zone of the flame, and only surface growth is applied to them in the post-nucleation zone. Coagulation was thus only taken into account up to the point of transition as it only affects the aggregate structure but has no influence on the shape of individual primary particles.

The simulations were initiated in the nucleation zone just prior to the maximum in the particle number density at 17.5 ms. The mean particle diameter at this instant of time was assigned to the collector particle. In the first step of the Monte-Carlo simulations, a candidate particle having a size in the interval of D_i and $D_i + \Delta D$ is selected at time t from the particle ensemble with a probability

$$P(D_i + \Delta D, t) = \int_{D_i}^{D_i+\Delta D} \beta_{D_i,D_j}(t) N_{D_i}(t)\,\mathrm{d}D \Big/ \int_{D_0}^{D_{\max}} \beta_{D_i,D_j}(t) N_{D_i}(t)\,\mathrm{d}D, \quad (4)$$

where D_i is the diameter of the candidate particle, ΔD is a small interval chosen as 0.01 nm, $\beta_{D_i,D_j}(t)$ is the coagulation kernel for the collector particle of known size D_j and the candidate particle of size D_i, N_i is the number density of the candidate particle of size D_i, D_0, and $D_{\max}$ are the diameters of the smallest and largest particles in the distribution of candidate particles, respectively. $N_{D_i}(t)$ was obtained from Eq. (3) using the pre-calculated parameters interpolated at time t.

After the candidate particle is selected, it is attached to the collector particle along a random trajectory. In the employed algorithm [20,21], all particles are treated as union of balls and this allows a detailed three-dimensional description of the shape of the collector particle. After the coagulation event is executed, time is incremented by Δt equal to the inverse of the average coagulation rate depending on the size of the collector particle.

Next, based on a time splitting technique, surface growth is applied to the collector particle for the same time increment Δt with the growth rate obtained from the pre-calculated results of the flame simulation described in Section 2.1. Surface growth is modeled as a uniform increase of the radii of all balls comprising the collector particle. The same procedure is then repeated at $t + \Delta t$ until the predefined transition time is reached, and only surface growth is applied for the remaining simulation time.

At all time steps, the shape of the collector particle was evaluated by calculating its fractal dimension D_f, radius of gyration, collision diameter, surface area, volume, and the shape descriptor d [21]. The shape descriptor was taken as the main measure for particle sphericity. It is defined as the normalized surface area to volume ratio of a particle

$$d = \ln(S/S_0)/\ln(V/V_0), \quad d \in [2/3, 1], \quad (5)$$

where S_0 and V_0 are the surface area and volume, respectively, of the collector particle at the start of the simulation. In the limit of a sphere, d takes a value of 2/3 while it is unity for an aggregate comprised of a chain of spheres of size V_0.

It is important to note that all candidate particles are assumed to be spheres. Also, since the premise of our study is to track only a single particle, aggregate–aggregate collisions were not consid-

ered. In the region before and during transition, which we are focusing on, aggregate–sphere collisions constitute the majority of all collisions. Aggregate–aggregate "coagulation" in the post-nucleation zone, while defining the overall aggregate geometry, has little effect on the shape of its constituent primary particles. The inclusion of aggregate–aggregate collisions should thus not affect the principal conclusion of the present study.

3. Results and discussion

A laminar premixed flame of ethylene and air was investigated (pressure 10 bar, C/O-ratio 0.673). This flame was selected since it serves as a point of comparison to previous studies that investigated this particular flame [20–22,25,30]. The flame structure and the distribution of soot particles were computed as described above. The calculated soot particle number density and volume fraction along with the corresponding experimental measurements [34] are shown in Fig. 1. Good agreement between the measured and calculated values of soot volume fraction was achieved with the detailed kinetic soot model. This indicates that the soot mass growth rates supplied to the Monte-Carlo simulations were well captured.

The size distribution computed using Eq. (1) is plotted in Fig. 2, where $n(D)$ is defined in Eq. (2). The initial size distribution closely resembles the shape of a power-law function. Due to simultaneous nucleation and coagulation, starting from 18 ms, the distribution can be divided into two parts, a power-law distribution at small sizes and a log-normal distribution for particles with larger diameters. The distributions shown in Fig. 2 could very accurately be fitted by Eq. (3). Soot particle size distributions exhibiting a similar shape were recently measured in premixed laminar flames by Zhao et al. [35].

From the results shown in Fig. 2, the number of small particles, i.e., the number of particles in the power-law part of the size distribution or par-

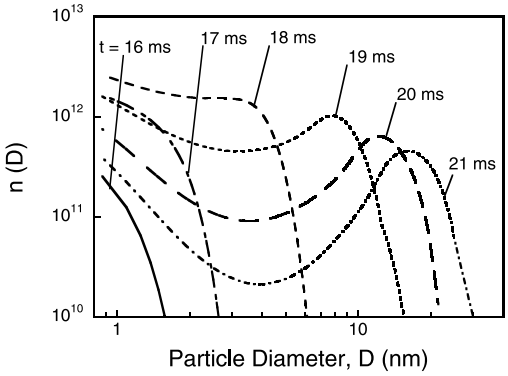

Fig. 2. Evolution of the size distributions of soot particles in the investigated laminar premixed flame.

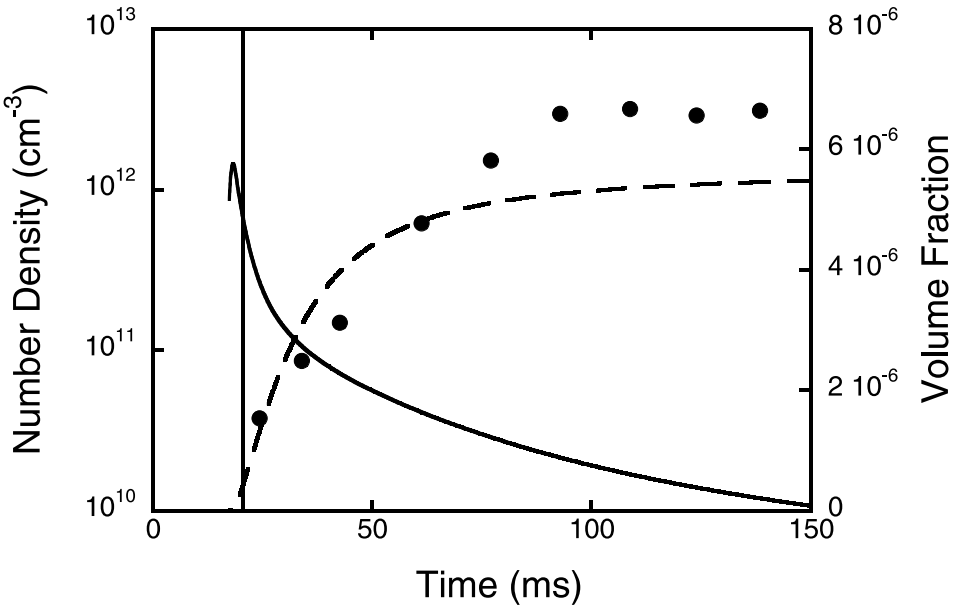

Fig. 1. Soot particle number density (solid line) and soot volume fraction (dashed line) as functions of residence time in a laminar premixed ethylene/air flame obtained with a detailed kinetic model. Only values for $t > 17.5$ are shown, corresponding to the start of the Monte-Carlo simulations. Also shown are measurements of soot volume fraction (symbols) taken from [34]. The horizontal line indicated the time of transition, $t = 20.5$ ms.

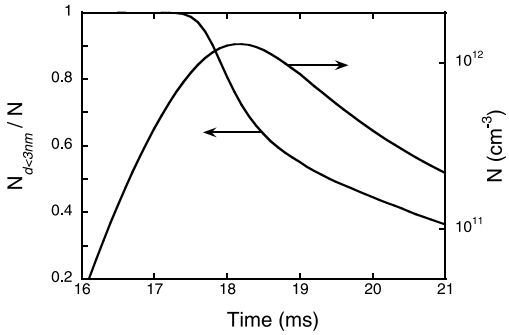

Fig. 3. Total particle number density and the fraction of particles with diameters smaller than 3 nm as functions of residence time obtained from the size distributions shown in Fig. 2.

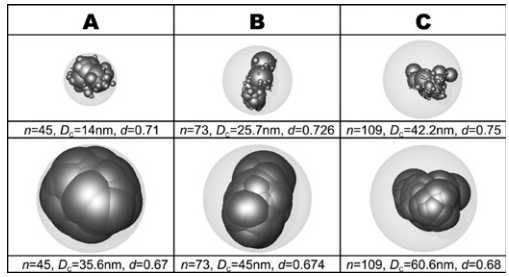

Fig. 4. Snapshots of primary particles at the time of transition, 20.5 ms, and the final simulation time, 220 ms. Shown are three different samples differing in their final values of d. (A) A typical case while (B) and (C) are extreme cases in terms of size and deviation from spherical shape.

ticles with $d < 3$ nm, was calculated and displayed in Fig. 3. After the peak in the total particle number density, the number of small particles is reduced rapidly due to coagulation and the drop in the nucleation rate. At 20.5 ms, the number of small particles has decreased to less than a third of its peak value. Balthasar and Frenklach [22] recently investigated the transition from coalescent to aggregate growth using a kinetic soot model based on the method of moments in the same flame as simulated here. It was found that particles, on average, started to deviate from spherical shape at around 20.5 ms. This behavior was attributed to a depletion of small particles, and it is confirmed by the present results, those depicted in Fig. 2. From this point in residence time, the particle ensemble is dominated by larger particles in the log-normal part of the distribution. Coagulation between large particles becomes prevailing and leads to the formation of aggregates.

According to the above considerations, Monte-Carlo simulations of the growth of primary soot particles were conducted. The trajectory of the collector particle was calculated starting at 17.5 ms, which corresponds to the main nucleation zone in the flame. The collector particle was initially assumed to be spherical and subjected to coagulation with candidate particles and surface growth up to the point of transition at 20.5 ms while only surface growth was applied thereafter. Snapshots of candidate particles obtained in this manner are depicted in Fig. 4. The upper panel of Fig. 4 displays the collector particles at the point of transition while the lower panel shows the same particles at the final simulation time. Also given is the number of candidate particles n comprising the collector particle, the collision diameter D_C, and the shape descriptor d. Three different collector particles were selected from a total of 5000 simulations. The particles differ in their final value of shape descriptor d as well as their diameters and represent limiting cases in terms of their sphericity.

Particle A in Fig. 4 is a representative example of the bulk of collector particles obtained in the simulations. It consists of 45 individual candidate particles collected over the time period prior to the point of transition and has a collision diameter of 14 nm at the point of transition. Its shape with a shape descriptor value of $d = 0.71$ deviates substantially from that of a sphere. However, it can also be seen that the core particles have already been "fused" by surface growth even though surface growth is rather small in this part of the flame.

The mean size of the candidate particles making up collector A is 1.5 nm at the respective times of collision. The size of the biggest candidate particle collected is 4.5 nm. The mean candidate particle diameter averaged over the whole ensemble at 20.5 ms is 7 nm. Comparing the diameters of the selected candidate particles with the size distribution depicted in Fig. 2 indicates that all candidate particles originate from its power-law part, namely they are recently incepted particles. The use of a realistic distribution of candidate particles thus significantly reduces the size of selected candidate particles as compared to the mean particle diameter. The degree of aggregation of collector particles at the point of transition is reduced, and the recovery of sphericity due to surface growth in the post-nucleation zone is facilitated. At the final simulation time, particle A reaches an almost perfectly spherical shape, as shown in the lower panel of Fig. 4. Its final diameter of 35.6 nm compares well with experimentally determined values of primary particle diameters found in flames burning under similar conditions [36].

Particles B and C, also shown in Fig. 4, reveal somewhat different features in terms of size and shape as compared to particle A. Their shape descriptors both at the transition and final times are higher than that of particle A. In addition, particle C represents the largest particles obtained in the simulations. For both collector particles B

and C, the mean size of candidate particles is roughly equal to that found for particle A. However, close inspection of Fig. 4 reveals that the maximum size of the constituent candidate particles is much larger. Collector B contains, in addition to the very small candidate particles, also two subparticles of diameters of around 11 nm. These subparticles were both added to the same edge, which led to a prolonged shape of the collector at transition time. While surface growth is able to bury gaps between the individual particles, the prolonged shape is evidently conserved until the final simulation time.

The number of large candidate particles within collector C is even higher than that for collector B, i.e., five subparticles of around 10 nm. The diameter of particle C is thus much larger than the diameters of particles A and B. Also, its shape descriptor d is rather high at transition time. However, as for the particles A and B, surface growth markedly increases the sphericity of the particle in the post-nucleation zone.

The inspection of particles A–C clearly confirms the results of previous studies [20,21] that the presence of small particles is essential for the formation of spherical primary particles. The use of a realistic size distribution is thus important. Small particles are present as long as nucleation is active and are scavenged rapidly once nucleation stops. If the majority of candidate particles added to the collector are small, surface growth will be able to bury the gaps between the particles and thus primary particles become spherical. If the distribution is highly populated with small particles, they will always form the bulk of selected candidate particles due to the large nonlinear size dependence of the coagulation kernel.

After inspecting individual particle histories, integral quantities averaged over all 5000 simulations were investigated. Figure 5 shows the mean fractal dimension $\langle D_f \rangle$ and the mean shape descriptor $\langle d \rangle$ as functions of residence time. Since the collector particles are assumed to be spherical at the start of the simulation, $\langle D_f \rangle$ and $\langle d \rangle$ have the initial values of 3 and 2/3, respectively. In the initial part of the flame, the fractal dimension decreases rapidly due to coagulation. It passes through a minimum of 2.35 at the point of transition, increases subsequently due to surface growth, and reaches a final value of 2.9. The evolution of the shape descriptor exhibits a similar behavior in terms of its inverse value. The final value of $\langle d \rangle = 0.675$ is only slightly higher than that of a sphere. This demonstrates that, similar to the previous results [20,21], the current model is able to predict the spherical shape of primary particles.

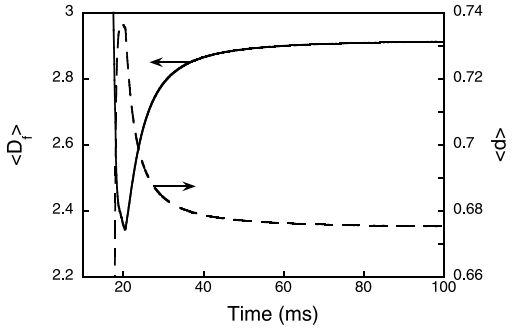

Fig. 5. Mean fractal dimension $\langle D_f \rangle$ and mean shape descriptor $\langle d \rangle$ of collector particles as functions of residence time averaged over 5000 simulations.

Figure 6 shows the size distribution of collector particles at three different points in time. It was found that the distributions obey a log-normal form throughout the entire flame. This is confirmed by fitting log-normal distributions to the simulated size distributions, also shown in Fig. 6. The calculated log-normal shape of the primary particle distribution agrees well with the experimental findings [37,38].

To examine the correlation between size and shape, the distribution of particles is displayed in Fig. 7 as a function of diameter and shape descriptor d for three different residence times. The distribution in d is initially rather broad, indicating a large range of particle shapes. After the transition, surface growth narrows the distribution. Finally, it becomes nearly mono-disperse with respect to d for particles of same size. It is also interesting to note that there is a clear correlation between shape descriptor and particle size in the distribution calculated at 100 ms. The final shape of large collector particles is found to be less spherical than that of small particles. The particles shown in Fig. 4 support this correlation.

Combining the results of the present and previous [20,21] studies, we can describe particle aggregation and transition from coalescent to aggregate growth in premixed laminar flames as follows. In the nucleation zone, the particle ensemble is dominated by small newly incepted particles but also

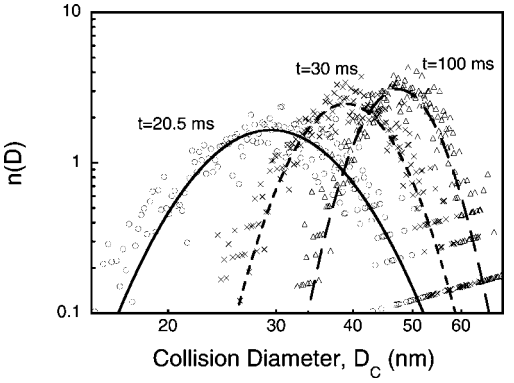

Fig. 6. Size distribution of collector particles at different residence times (symbols). Also shown are fitted log-normal distributions (lines).

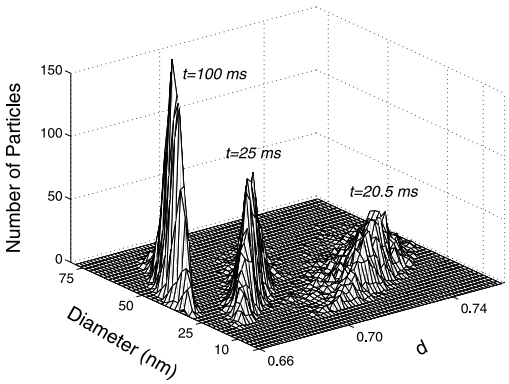

Fig. 7. Distribution of collector particles as a function of collision diameter and shape descriptor d at three different residence times.

large particles are present due to coagulation. These large particles coagulate preferably with the smaller particles to form particles as depicted in Fig. 4. Surface growth, although still relatively small in this region of the flame, fills to some extent the small gaps in the larger particles. Once nucleation stops these larger particles begin colliding with other large particles forming aggregates. Thus, the larger particles appearing at the point of transition can be regarded as primary particles. The point of transition divides the two zones of the flame and is governed by the cessation of nucleation. In the post-nucleation zone, surface growth continues to enhance the sphericity of the primary particles.

In the flame investigated in the present study, nucleation decreases rapidly after its maximum, which characterizes the transition to aggregation. In contrast to this, continuous nucleation leading to a constant presence of small particles has been observed in some laminar premixed flames, cf. [35]. Although the criteria for the onset of ensemble aggregation may be different for such situations, aggregate formation will still occur as shown in [22].

4. Conclusions

The effect of a realistic particle size distribution on the morphology of primary soot particles was investigated by simulating trajectories of single particles in a premixed laminar flame. The flame was divided into a nucleation-dominated zone early in the flame and a post-nucleation zone governed by surface growth. The transition between the two zones was taken from the results of a previous study [22]. In the nucleation zone of the flame, particles were allowed to grow by coagulation and surface growth while only surface growth was applied in the post-nucleation zone. This is motivated by the fact that coagulation in the second part of the flame does not affect the shape of primary particles but merely determines the final fractal nature of aggregates.

The candidate particles available for coagulation were obtained from a size distribution of particles calculated from the Smoluchowski master equations with additional source terms for surface growth and nucleation. It was found that the particle size distribution in the nucleation zone of the flame can be divided into two parts: the newly incepted particles that dominate the distribution and a small fraction of larger particles formed by coagulation. The evolution of these larger particles was simulated by a time-dependent Monte-Carlo method [20,21,33].

In the first part of the flame, the larger particles coagulate almost exclusively with small particles due to a higher collision frequency forming slightly aggregated particles. The use of a realistic size distribution reduces the mean size of candidate particles selected for coagulation and hence the degree of aggregation of primary particles at the point of transition. Once nucleation has ceased, the small particles are rapidly scavenged by the large particles and transition occurs. From this point in the flame onward, the larger particles can be regarded as primary particles. It was found that surface growth acting on the particles in the post-nucleation zone was able to recover the spherical shape of the primary particles.

The present results provide further support of the mechanism of transition from coalescent coagulation to fractal-like growth identified in previous studies [20–22] and demonstrate the significance of small particles on the formation of spherical primary particles.

Acknowledgments

The authors thank Pablo Mitchell for his help with the Monte-Carlo code. The support of the Alexander-von-Humboldt Foundation, Germany, to M.B. is gratefully acknowledged. M.F. acknowledges support from the Office of Energy Research, Office of Basic Energy Sciences, Chemical Division of the US Department of Energy, under Contract No. DE-AC03-76SF00098.

References

[1] S.N. Rogak, R.C. Flagan, H.V. Nguyen, *Aerosol Sci. Technol.* 18 (1993) 25–47.
[2] Ü.Ö. Köylü, G.M. Faeth, T.L. Farias, M.G. Carvalho, *Combust. Flame* 100 (1995) 621–633.
[3] A.V. Filippov, M. Zurita, D.E. Rosner, *J. Colloid Interf. Sci.* 229 (2000) 261–273.
[4] C.M. Sorensen, *Aerosol Sci. Technol.* 35 (2001) 648–687.

[5] D.B. Kittelson, *J. Aerosol Sci.* 29 (1997) 575–588.
[6] R.D. Mountain, G.W. Mulholland, *Langmuir* 4 (1988) 1321–1326.
[7] C.M. Megaridis, R.A. Dobbins, *Combust. Sci. Technol.* 63 (1989) 152–167.
[8] B.S. Haynes, H.G. Wagner, *Prog. Energy Combust. Sci.* 7 (1981) 229–273.
[9] D.W. Dockery, C.A. Pope, X. Xu, J.D. Spengler, J.H. Ware, M.E. Fay, J.B.G. Ferris, F.E. Speizer, *J. Med.* 329 (1993) 1753–1759.
[10] C.A. Pope, M.J. Thun, M.M. Namboodiri, D.W. Dockery, J.S. Evans, F.E. Speizer, J.C.W. Heath, *Am. J. Respir. Crit. Care Med.* 151 (1995) 669–674.
[11] K. Kinoshita, *Carbon, Electrochemical and Physiochemical Properties.* Wiley, New York, 1988.
[12] G. Ulrich, N.S. Subramanian, *Combust. Sci. Technol.* 17 (1977) 119.
[13] W. Koch, S.K. Friedlander, *J. Colliod Interf. Sci.* 140 (1990) 419–427.
[14] G. Prado, J. Jagoda, K. Neoh, J. Lahaye, *Proc. Combust. Inst.* 18 (1981) 1127–1136.
[15] Y. Xiong, S.E. Pratsinis, *J. Aerosol Sci.* 24 (1993) 283–300.
[16] R.A. Dobbins, *Combust. Flame* 130 (2002) 204–214.
[17] B.L. Wersborg, J.B. Howard, G.C. Williams, *Proc. Combust. Inst.* 14 (1973) 929–938.
[18] J.B. Howard, J.P. Longwell, in: M. Cooke, A.J. Dennis (Eds.), *Polynuclear Aromatic Hydrocarbons: Formation, Metabolism, and Measurements.* Battelle, Columbus, OH, 1983, pp. 27–62.
[19] G.W. Smith, in: J. Lahaye, G. Prado (Eds.), *Soot in Combustion Systems and Its Toxic Properties.* Plenum, New York, 1983, pp. 163–170.
[20] P. Mitchell, M. Frenklach, *Proc. Combust. Inst.* 27 (1998) 1507–1514.
[21] P. Mitchell, M. Frenklach, *Phys. Rev. E* 67 (2003) 061407.
[22] M. Balthasar, M. Frenklach, in preparation, 2004.
[23] R.J. Kee, J.F. Grcar, M.D. Smooke, J.A. Miller, *A Fortran Program for Modeling Steady Laminar One-dimensional Premixed Flame*, Tech. Rep. SAND85-8240, Sandia National Laboratories, 1990.
[24] K.L. Revzan, N.J. Brown, M. Frenklach, unpublished. Available from: <http://www.me.berkeley.edu/soot/codes/codes.html>.
[25] J. Appel, H. Bockhorn, M. Frenklach, *Combust. Flame* 121 (2000) 122–136.
[26] H. Wang, M. Frenklach, *Combust. Flame* 110 (1997) 173–221.
[27] M. Frenklach, H. Wang, in: H. Bockhorn (Ed.), *Soot Formation in Combustion: Mechanisms and Models.* Springer-Verlag, Heidelberg, 1994, pp. 165–192.
[28] M. Frenklach, *Chem. Eng. Sci.* 57 (2002) 2229–2239.
[29] M.V. von Smoluchowski, *Z. Phys. Chem.* 92 (1917) 129.
[30] A. Kazakov, M. Frenklach, *Combust. Flame* 114 (1998) 484–501.
[31] M. Frenklach, *Phys. Chem. Chem. Phys.* 4 (2002) 2028.
[32] P.N. Brown, G.D. Byrne, A.C. Hindmarsh, *SIAM J. Sci. Statist. Comput.* 10 (1989) 1038–1051.
[33] P. Mitchell, Ph.D. Thesis, University of California, Berkeley, 2001.
[34] H. Jander, Studied in Ref. [30], 1992.
[35] B. Zhao, Z. Yang, M.V. Johnston, H. Wang, A.S. Wexler, M. Balthasar, M. Kraft, *Combust. Flame* 133 (2003) 173–188.
[36] H. Hanisch, H. Jander, T. Pape, H.G. Wagner, *Proc. Combust. Inst.* 25 (1995) 577–584.
[37] Ü.Ö. Köylü, G.M. Faeth, *J. Heat Transfer* 115 (1993) 409–417.
[38] T. Heidermann, H. Jander, H.G. Wagner, *Phys. Chem. Chem. Phys.* 1 (1999) 3497–3502.

Comments

Jay Boris, NRL, USA. Is there any evidence for or do you expect any site-dependent or geometry dependent effects in the soot particle agglomeration?

Reply. The model employed in the present work ([20-22] in paper) can be viewed as a "first-order" approximation to the "reality": individual constituent particles are assumed to be perfect spheres with a uniform mass density and a uniform rate of expansion (i.e., surface growth). It is rather remarkable that such a simple model is able to capture so closely the geometric properties of soot particles collected in experiment. It is reasonable to expect that the outcome of particle collision may depend on the chemical state and geometry of the colliding surfaces. It would be of interest to examine the contribution of these phenomena when their physical details become known.

•

Elaine Oran, NRL, USA. What are the effects of varying background initial pressure (< or > 10 bar)? What are the effects of gravity?

Reply. We did not study the effect of gravity in the present work. The effect of pressure was investigated in our previous study [22 in paper].

•

Paul Roth, Universität Duisburg-Essen, Germany. Do you expect an effect of electrically charged particles in your wavelength coagulation calculations?

Reply. Balthasar et al. [1] investigated the effect of thermo-ionization on soot formation in laminar premixed flames using the method of moments. They found that the effect of particle charging on soot volume fraction and number density is small in a typical sooting laminar premixed flame. Nevertheless, it is not unreasonable to expect an effect of charging on the structure of aggregates. This effect was however not investigated in the current study.

Reference

[1] M. Balthasar, F. Mauss, H. Wang, *Combust. Flame* 129 (2002) 204–216.

•

Daniel E. Rosner, Yale University, USA. Especially in the nano-particle domain, I presume that your promising results for the case of surface growth do not preclude an important role for "rival" coalescence/sintering mechanisms (not only viscous flow, but also surface-diffusion [1]).

If the "saddle-shaped" region where two particles touch was either: a.) a preferred site for growth (as in the case of capillary condensation) or, alternately b.) relatively "inaccessible" (leading to locally reduced growth rates), how would this affect your principal conclusions?

Reference

[1] Y. Xing, D.E. Rosner, *J. Nanoparticle Res.* 1 (1999) 277–291.

Reply. The present model does not preclude incorporation of additional phenomena (see our reply above to Jay Boris' comment). This being said, however, it is these authors' opinion that neither direct evidence nor theoretical reasoning exists for the sintering mechanism (due to viscous forces) to be considered an important factor in soot particle aggregation. The sintering phenomena can be envisioned for materials like silicon, silica, or titania, those composed of atoms or small molecules. Such materials possess a clearly defined melting point, with melting temperature decreasing with the reduction of particle size. Under these conditions, one can indeed envision an inter-diffusion of atoms or small molecules between the two colliding particles. In contrast, soot (like graphite or diamond) does not undergo melting, at any temperature. Whatever the details are, the internal structure of soot particles is comprised of polyaromatic-size molecular units. While some realignment of these aromatic units is known (and usually referred to as annealing), their long-range inter-penetrating motion is unlikely, and has not been demonstrated, neither experimentally nor theoretically. Still, some rearrangement of aromatic units (as suggested, e.g., in [20 in paper] for collisions of small PAH clusters) and the influence of surface diffusion (perhaps of cyclopentha groups [1]) is very likely, and these questions, along with the subject of "necking" (the "saddle-shaped" region), should be of interest to investigate. It is possible, however, that all such factors might end up being secondary to the simple "geometric effect" revealed by the present model [20–22 in paper].

Reference

[1] M. Frenklach, C.A. Schuetz, J. Ping, *Proc. Combust. Inst.* 30 (2005) 1389–1396.

•

Richard Dobbins, Brown University, USA. Examination of TEM images of young soot particles reveals some irregularly shaped entities like those in your modeling studies. A more interesting case is the formation of filose aggregates of the more carbonaceous soots that are chemically and physically distinct from the isolated young spheroidal particles. The distinctive morphology of the aggregates results from their non-coalescent collisions. They have a lower H/C ratio from the carbonization reactions in the higher temperature regions of the flame, an attendant higher particle density near 1.85 gm/ml, and a higher complex portion of the refractive index. Carbonaceous soots display Bragg diffraction of X-rays from which crystal lattice dimensions are derived [1]. The diffraction effects from carbonaceous soots are also displayed in dark field TEM [1, 2]. Oberlin [3] first explained these "bright domains" in DFTEM of kerogens to result from stacking of planar multi-ring PAH molecules. Noteworthy are the faint Bragg diffraction effects in DFTEM [1, 2] even in young soot particles.

References

[1] H.X. Chen, R.A. Dobbins, *Combust. Sci. Tech.* 159 (2000) 109–128.
[2] R.L. Vander Wal, *Combust. Sci Tech.* 126 (1997) 333–357.
[3] A. Oberlin, *Carbon* 22 (1984) 521–541.

Reply. The objective of our modeling work ([20–22] in paper) has been to study the phenomenon of transition from "spherical" to "fractal" particles, and to identify the factors governing this transition. The results obtained thus far indicate that, irrespective of physical details and material structure, the governing factor affecting the transition is basically "geometric" in nature: relative sizes of the colliding particles, and hence the interplay among nucleation, collision, and surface growth rates. While, unfortunately, there are no direct measurements documenting the instant of transition, the model is demonstrated to reproduce closely the particle shapes reported in the literature, both the small, spheroidal particles and the larger, fractal-like aggregates.